RESEARCH ARTICLE

Analysis of drying characteristics and quality of Star Anise (*Illicium verum*) using microwave vacuum and hot air combined drying

Yongfu Liu[1, †], Xiaoting Zhou[2, †], Xiaoli Pan[1, 3, 4, *], Wenyan Fan[2, *], Guimei Yang[5], Wangxin Yu[1], Weisheng Hong[1]

[1]School of Physical and Telecommunication Engineering, Yulin Normal University, Yulin, Guangxi, China. [2]Yulin Center for Food and Drug Control, Yulin, Guangxi, China. [3]Guangxi Colleges and Universities Key Lab of Complex System Optimization and Big Data Processing, Yulin Normal University, Yulin, Guangxi, China. [4]Center for Applied Mathematics of Guangxi, Yulin Normal University, Yulin, Guangxi, China. [5]Fangchenggang Agricultural Machinery Service Center, Fangchenggang, Guangxi, China.

Received: September 12, 2023; **accepted:** November 5, 2023.

Star anise, rich in effective active constituents, is extensively employed in the pharmaceutical and food industries. The drying temperature can irreversibly damage these constituents. To enhance the drying quality and efficiency, this study undertook experiments using three drying methods on star anise including microwave vacuum drying, hot air drying, and a combination of microwave vacuum and hot air drying. The research examined the impacts of varying drying conditions on the drying characteristics of star anise, the moisture diffusion coefficient, and the primary component contents (anethole and shikimic acid). Models were separately established for microwave vacuum and hot air thin-layer drying kinetics including Lewis, Weibull distribution, two-term exponential, Wang, and Singh models, and a Weibull distribution model for combined microwave vacuum-hot air drying. The results indicated that drying with microwave vacuum and hot air primarily proceeded in a falling rate drying phase, whereas combined microwave vacuum and hot air drying encompassed both falling rate and constant rate stages. The effective moisture diffusion coefficients (D_{eff}) for microwave vacuum drying and hot air drying of star anise ranged from 3.4423E-07 to 8.8239E-07 m^2/s and 2.0386E-08 to 8.8239E-07 m^2/s, respectively, while the D_{eff} for combined microwave and hot air drying ranged from 2.8683E-07 to 4.8014E-07 m^2/s and 7.9516E-8 to 2.0964E-7 m^2/s, respectively. Evidently, segmented combined drying facilitated more convenient moisture diffusion, and both coefficients increased with microwave power and hot air temperature. During the microwave vacuum and hot air drying processes, both the Wang and Singh models and the Weibull distribution models showed good fitting effects. The Weibull distribution model could effectively predict the drying behavior of segmented microwave vacuum and hot air drying of star anise. In comparison with hot air drying time, combined microwave vacuum and hot air drying shortened the drying time by 30% to 92%. Considering quality and energy consumption, a microwave power of 2,000 W, a conversion moisture content of 30%, and a hot air drying temperature of 45°C were selected as the optimal drying parameters. Employing the combined microwave vacuum and hot air drying technique, this study, with a focus on drying efficiency and high quality, provided a scientific and theoretical foundation for the drying production of star anise, which represented a significant breakthrough in the traditional drying methods of star anise as a medicinal herb.

Keywords: Star Anise; drying characteristics; drying kinetics models; microwave vacuum; hot air drying; quality.

[*]**Corresponding authors:** Xiaoli Pan, School of Physical and Telecommunication Engineering, Yulin Normal University, Jiaoyudong 1303, Yulin, Guangxi 537000, China. Email: 349230222@qq.com. Wenyan Fan, Yulin Center for Food and Drug Control, No.30 Zhitang Street, Minzhu Middle Road, Yulin, Guangxi 537000, China. Email: 2740876952@qq.com.

[†]These authors contributed equally.

Introduction

Star anise (*Illicium verum*), also known as Chinese star anise or badiam, is predominantly found in regions such as Guangdong, Guangxi, and Yunnan in China. After undergoing drying processing, it serves as a seasoning and is recorded in the Pharmacopoeia for its medicinal value. Star anise exhibits anti-inflammatory, analgesic, warming, and pain-relieving properties that are utilized in treating cold-induced abdominal pain, kidney weakness, chills with vomiting, and bloating. It is the sole proven remedy against avian influenza, with shikimic acid derived from star anise being the key ingredient in the Tamiflu medication, which effectively prevents the disease [1]. Current drying practices for star anise include sun-drying, fixing and drying, hot air drying, and sulfur fumigation, all of which are simple methods. Problems arise during periods of heavy rain, leading to decay if drying is not prompt. General quality control is lacking, and excessive drying temperature or time can result in discoloration and decomposition of essential oils, affecting flavor and medicinal efficacy [2]. Hence, the selection of an appropriate drying method is crucial for preserving active constituents in star anise.

Microwave vacuum drying is an innovative technology combining the efficiency of microwaves with the low-temperature characteristics of vacuum conditions. It retains the active components of the material, and the vacuum environment with minimal oxygen content has achieved favorable results in agricultural products and traditional Chinese medicine processing, including pumpkin [3], lotus seeds [4], potatoes [5], beef [6], Panax notoginseng [7], and Angelica [8]. Microwave drying greatly accelerates star anise drying, but incorrect parameter choices can lead to scorching and local charring [9, 10]. Hot air drying is a processing method widely adopted in current production. However, overly high drying temperatures and prolonged drying times can result in the loss of thermally sensitive substances and active ingredients in star anise, even though this method offers the advantages of low equipment costs and simple installation and operation.

Research has indicated that heat-sensitive substances may be lost during prolonged microwave drying, possibly due to local overheating at edges or pointed areas, causing volatilization and quality degradation [11]. Especially during the final drying stage, when moisture content drops, uneven microwave distribution leads to a rapid internal temperature rise. To alleviate overheating, this study utilized a combination method by applying microwave vacuum drying to a certain moisture content followed by hot air drying. This approach has been effective in studies on mango slices [12] and cranberries [13]. The drying process is a complex heat and mass transfer process, and to date, no specific theory has been formed. Building a model for the drying process allows for the prediction of drying time, moisture ratio, drying rate, and other parameters based on the moisture ratio's changing pattern. The thin-layer drying mathematical model can satisfactorily simulate the drying process's moisture change pattern. This study applied microwave vacuum, hot air, and combined microwave vacuum-hot air drying methods to star anise, fitted a thin-layer drying model suitable for the experimental data, explored star anise's drying characteristics under varying power density, hot air temperature, and conversion moisture content conditions, employed the Weibull distribution function for the investigation of water diffusion properties and heat and mass transfer mechanisms during drying, calculated effective moisture diffusion coefficients and activation energy, and analyzed the combined drying conditions' effect on trans-anethole and shikimic acid. This research provided theoretical support for the prediction and control of star anise drying.

Materials and Methods

Hot air drying

Table 1. Experimental design and parameters.

Number	Microwave Power (W)	Hot Air Temperature (℃)	Conversed Moisture Content (%)
1	1000	55	30
2	3000	55	30
3	2000	45	30
4	2000	45	50
5	2000	65	30

Star anise was harvested from Liuwandashan, Yulin, Guangxi, China by selecting uniformly sized, consistent maturity, pest-free, and undamaged samples as experimental materials. All samples were preserved at 4°C with an initial moisture content of 77.3%. Traditional hot air drying temperatures are around 50°C with processing sites having drying temperatures around 60°C and infrared radiation drying yielding optimal quality at 70°C [2]. This study employed KL-2D-6 Hot Air Drying Oven (Guangzhou Kailong Microwave Equipment Co., Ltd., Guangzhou, Guangdong, China) with the drying temperatures setting at 45, 50, 55, 60, and 65°C. The oven was preheated to the specified temperature, and 1,000 g of uniformly sized star anise was spread on a metal screen with a wind speed set at 1.2 m/s. Samples were taken out and weighed every 30 minutes until the end of the experiment with moisture content below 15%. Each experiment was repeated three times for an average value.

Microwave vacuum drying

The WZD6 Microwave Vacuum Sterilizing Furnace (Nanjing Sanle Microwave Technology Development Co., Ltd., Nanjing, Jiangsu, China) was employed in this study. 1,000 g of star anise were evenly distributed across six rotating baskets within the microwave vacuum furnace. Drying experiments were conducted at various microwave power levels including 1,000 W, 1,500 W, 2,000 W, 2,500 W, and 3,000 W within a relative vacuum range of -80 to -92 kPa. The top of the vacuum chamber was equipped with a temperature acquisition device to collect real-time surface temperatures of the star anise inside the rotating baskets. The temperatures were displayed on an LCD screen and stored. Samples were taken out and weighed every 5 minutes with each experiment being repeated three times to obtain an average value.

Microwave vacuum combined with hot air drying

A single-factor experimental design was employed for the combined microwave vacuum-hot air drying experiment. The specific experimental design and parameter values were presented in Table 1.

Determination of trans-anethole and shikimic acid content

The trans-anethole and shikimic acid contents were determined by using Agilent-1260 High-Performance Liquid Chromatography including a quaternary pump, DAD detector, online degasser (Agilent Technologies, Santa Clara, CA, USA) and KQ-250DB CNC Ultrasonic Cleaner (Kunshan Ultrasonic Instruments Co., Ltd., Kunshan, Jiangsu, China). Approximately 0.5 g of the powdered sample was precisely weighed followed by the accurate addition of 25 mL of ethanol. The sample was subjected to ultrasonic treatment for 30 minutes and reweighed after cooling down. The lost weight was compensated with ethanol. After shaking well, the sample was filtered through a 0.45 μm microporous membrane and a precise volume of 1.0 mL of the filtrate was placed in a 10 mL volumetric flask. Ethanol was added to the mark, and the mixture was shaken well for use. Shikimic acid and trans-anethole obtained from National Institute for Food and Drug Control, Beijing, China were used as reference substances. Shikimic Acid Single Standard Reserve Solution was prepared by weighing 9.09 mg of shikimic acid control substance (with a percentage content of 98%) in

a 10 mL volumetric flask, achieving a concentration of 0.89082 mg/mL. Trans-Anethole Single Standard Reserve Solution was prepared by weighting 101.00 mg of trans-anethole control substance (with a percentage content of 100%) in a 10 mL volumetric flask, resulting in a concentration of 10.10 mg/mL. Mixed Standard Solution was prepared by precisely mixing 5 mL of Shikimic Acid Single Standard Reserve Solution and 0.5 mL of Trans-Anethole Single Standard Reserve Solution in a 10 mL volumetric flask, resulting in concentrations of 0.4454 mg/mL shikimic acid and 0.5050 mg/mL trans-anethole.

Drying mathematical model

Four empirical models were selected from classical models to fit the drying curve of star anise. The goodness of fit for the mathematical model was evaluated by using the determination coefficient (R^2), chi-square value (χ^2), and root-mean-square error (*RMSE*). A lower chi-square and *RMSE* value along with a higher determination coefficient indicated a better model fit [14]. The moisture ratio (*MR*) represented the change in moisture content of the material during the drying process, and its calculation formula could be simplified as:

$$MR = M_t / M_0 \tag{1}$$

where M_t was the moisture content of star anise at time t (g/g). M_0 was the initial moisture content of star anise (g/g). The drying rate D_R (kg/kg·min) measured the extent of change in star anise moisture over the time was calculated as follows:

$$D_R = -\left(m_{(t+\Delta t)} - m_t\right) / \Delta t \tag{2}$$

where $m_{(t+\Delta t)}$ and m_t were the moisture contents at time t+Δt, and t during the drying process (kg/kg).

$$R^2 = 1 - \frac{\sum_{i=1}^{N}\left(MR_{pre,i} - MR_{\exp,i}\right)^2}{\sum_{i=1}^{N}\left(\overline{MR_{pre,i}} - MR_{\exp,i}\right)^2} \tag{3}$$

$$\chi^2 = \frac{\sum_{i=1}^{N}\left(MR_{pre,i} - MR_{\exp,i}\right)^2}{N - n} \tag{4}$$

$$RMSE = \sqrt{\frac{\sum_{i=1}^{N}\left(MR_{pre,i} - MR_{\exp,i}\right)^2}{N}} \tag{5}$$

where $MR_{pre,i}$ was the i^{th} predicted moisture ratio in the drying test. $MR_{\exp,i}$ was the i^{th} experimental moisture ratio in the drying test. N was the number of experimental measurements.

Effective diffusion coefficient and activation energy

When the drying process was primarily controlled by the falling rate stage, Fick's diffusion equation was used to describe the drying characteristics with the simplified calculation equation as follows [15]:

$$\ln MR = \ln\frac{8}{\pi^2} - \frac{\pi^2 D_{eff} t}{4L^2} \tag{6}$$

where D_{eff} was the effective moisture diffusion coefficient (m²/s). L was the sample thickness (m) with a value of 0.005 m in this experiment. t was the drying time (min). The Arrhenius equation described the relationship between the effective diffusion coefficient and temperature, where activation energy represented the energy required to remove 1 mole of water, indicating the difficulty and energy consumption of drying. The internal water diffusion in star anise with respect to microwave power and hot air complied with the Arrhenius equation. The solutions to this equation provided the activation energy for different drying methods regardless of whether there was a strict falling rate stage during the drying process and was calculated as follows:

$$D_{eff} = D_0 \cdot \exp\left(-\frac{E_a \cdot m}{p}\right) \tag{7}$$

$$\ln D_{eff} = \ln D_0 - \frac{E_a}{R(T + 273.15)} \quad (8)$$

where D_0 was a constant of pre-exponential factor in the Arrhenius equation (m^2/s). *Ea* was material drying activation energy (kJ/mol). m was material mass (g). p was microwave power (W). R was the universal gas constant (8.314 J/mol·K. *T* was the hot air drying temperature (℃).

Results and discussion

Analysis of the drying kinetic characteristics of star anise

Drying is a crucial process in the processing of star anise. The examination of the drying curve helps select the correct drying method and parameters. The variations in moisture ratio for three drying methods of microwave vacuum drying, hot air drying, and a combination of microwave vacuum and hot air drying were shown in Figure 1. Within the microwave power range of 1,000 – 3,000 W, the drying time was significantly reduced. Compared to 1,000 W, the drying duration at 3,000 W was shortened by 59%. For hot air drying temperatures ranging from 45 to 65°C, the drying time at 65°C was 57% shorter than that at 45°C. The drying time for the segmented combined microwave vacuum and hot air drying was notably shorter than that of hot air drying alone. When the combined drying hot air temperature exceeded 55°C, the drying time was comparable to that of microwave vacuum drying. The drying rate curves were shown in Figure 2. It was evident that the higher the microwave intensity, the shorter the drying time (Figure 2A). The moisture molecules within star anise absorbed more microwave energy, thus facilitating rapid moisture migration. The rate curve of microwave vacuum drying revealed that, at a low microwave power of 1,000 W, the drying process was governed by a constant rate phase. The absorbed microwave energy was primarily utilized for the latent heat of vaporization necessary for water evaporation. During this phase, the material's moisture ratio exhibited a linear declining trend, and the drying rate remained stable. The constant rate phase lasted approximately 50 minutes, becoming the predominant factor. At a microwave power of 1,500 W, the drying rate was comprised of three segments including acceleration, brief constant rate, and deceleration, with the latter assuming the primary role. Brief periods of constant rate existed at 10 - 15 minutes and 20 - 25 minutes. As the microwave power increases to 2,000, 2,500, and 3,000 W, the acceleration phase was completed within 5 - 10 minutes, and the deceleration phase predominated. The drying time at 3,000 W was 62.5% shorter than that at 1,000 W, and the maximum drying rate had increased by 195.9%. The influence of microwave power on the drying process was thus significant. The drying rate curve for hot air drying was shown in Figure 2B with a peak drying rate of only 0.67%/min, which was a decrease of 96% compared to the maximum drying rate of 15.5%/min achieved with microwave vacuum drying, highlighting the significantly enhanced efficiency offered by microwave vacuum drying. The process was dominated by the deceleration phase. There was an initial acceleration phase lasting approximately 60 - 120 minutes followed by a prolonged deceleration phase. When the drying temperature was at its minimum, 45℃, a brief constant rate drying phase existed between 120 - 300 minutes, stabilizing at 0.28%/min. Hot air drying took longer and has a substantially reduced drying rate compared to microwave vacuum drying, which was attributed to the star anise's tough outer shell, which greatly impeded moisture evaporation. During conventional hot air drying, both temperature and moisture gradients transferred from the outside inward. Once the outer shell dried and hardened, internal moisture evaporation became difficult. The maximum drying rate for hot air drying was only 0.57%/min compared to 15.3%/min for microwave vacuum drying, signifying a remarkable difference. Utilizing microwave vacuum drying for hard-surfaced materials like star anise could substantially reduce drying time and conserve energy. The curves for combined

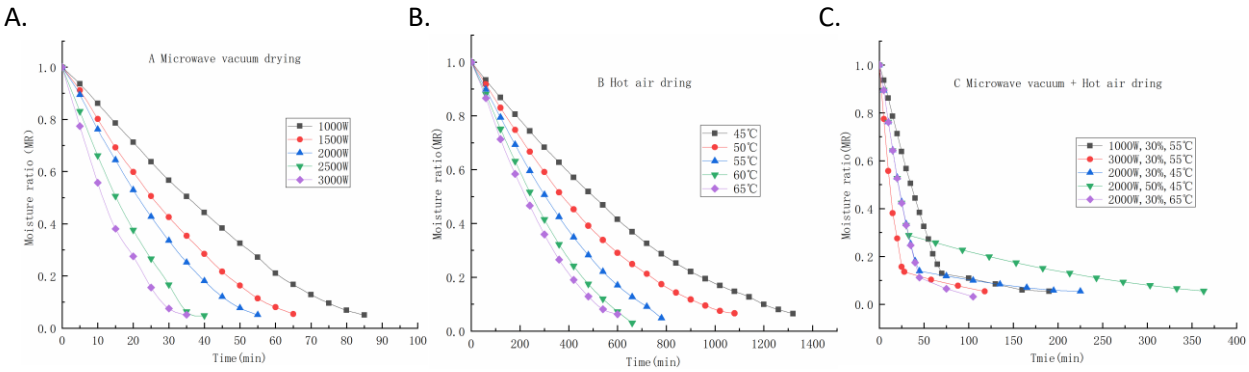

Figure 1. Variation in moisture ratio of star anise under different drying methods over the time. **A.** Microwave vacuum drying. **B.** Hot air drying. **C.** Microwave vacuum and hot air drying.

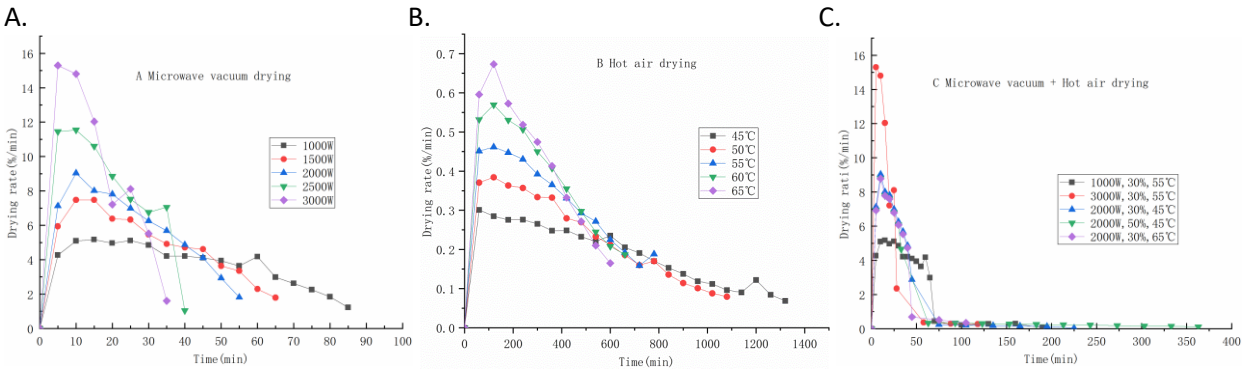

Figure 2. Drying rate curves of star anise under different drying methods. **A.** Microwave vacuum drying. **B.** Hot air drying. **C.** Microwave vacuum and hot air drying.

microwave vacuum and hot air drying indicated a reduction in drying time of over 1,000 minutes compared to hot air drying (Figure 2C). At the end of the deceleration phase in microwave vacuum drying, most of the free water in star anise had been removed, and the material's dielectric loss coefficient diminished, reducing the absorption of microwave energy. At this point, the total microwave energy absorbed by the star anise far exceeded the energy required to evaporate the moisture, resulting in a transient overheating, substantially affecting the content of heat-sensitive volatile oils. To resolve this issue, microwave vacuum drying was halted when the wet base moisture content reached 30% or more, transferring the star anise to a hot air dryer. Thus, combined microwave vacuum and hot air drying not only saved drying time but also prevented microwave overheating. The entire drying process was primarily controlled by the deceleration phase with the microwave portion of the combined drying following the same drying rate and moisture ratio trend as microwave vacuum drying alone. Only the hot air portion required analysis and model fitting. It was evident that the differences between the curves were pronounced during the microwave vacuum drying phase. Upon entering the hot air drying phase, the drying rates under different conditions were nearly identical. Even if the drying temperature was increased during the late drying stage, the drying rate remained virtually unchanged due to the hardening of the star anise's exterior and the residual bound water within the cells, which was challenging to remove.

Analysis of the optimal thin-layer drying model

Table 2. Fitting results of the star anise microwave vacuum drying model.

Model Name	Microwave Power (W)	Parameters	R^2	*RMSE*	χ^2
Lewis	1,000	k=0.02275	0.9589	0.06164	0.00402
	1,500	k=0.03094	0.9704	0.05244	0.00296
	2,000	k=0.03723	0.9678	0.05609	0.00343
	2,500	k=0.05245	0.9694	0.05604	0.00353
	3,000	k=0.06658	0.9851	0.03922	0.00176
Weibull distribution	1,000	a=44.2221, b=1.4342	0.9959	0.01892	4.0281E-4
	1,500	a=32.6585, b=1.3609	0.9975	0.01455	2.4711E-4
	2,000	a=27.2539, b=1.3958	0.9979	0.01363	2.2302E-4
	2,500	a=19.4735, b=1.3788,	0.9949	0.02122	5.7892E-4
	3,000	a=15.3820, b=1.2604,	0.998	0.01329	2.3576E-4
Two-term exponential	1,000	a=1.93147, k=0.03513	0.9927	0.02524	7.1692E-4
	1,500	a=1.88186, k=0.0465	0.9910	0.01879	4.0871E-4
	2,000	a=1.91645, k=0.05661	0.9959	0.01920	4.4238E-4
	2,500	a=1.89455, k=0.07836	0.9927	0.02568	8.4766E-4
	3,000	a=1.80369, k=0.09407	0.9975	0.01483	2.9339E-4
Wang and Singh	1,000	a=-0.0162, b=5.58323E-5	0.9984	0.01289	1.5718E-4
	1,500	a=-0.02277, b=1.2352E-4	0.999	0.009249	9.9778E-5
	2,000	a=-0.02722, b=1.7547E-4	0.9983	0.01218	1.7814E-4
	2,500	a=-0.03807, b=3.44645E-4	0.9984	0.01201	1.8528E-4
	3,000	a=-0.0503, b=6.5987E-4	0.9990	0.009331	1.16073E-4

Table 3. Fitting results of the star anise hot air drying model.

Model Name	Temperature (℃)	Parameters	R^2	*RMSE*	χ^2
Lewis	45	k=0.00155	0.9839	0.04139	0.00171
	50	k=0.00203	0.9848	0.03780	0.00139
	55	k=0.00258	0.9739	0.08573	0.00255
	60	k=0.0032	0.9695	0.05707	0.00326
	65	k=0.0035	0.9776	0.06154	0.00237
Weibull distribution	45	α=650.1896, β=1.2696	0.9984	0.01147	1.37743E-4
	50	α=498.9331, β=1.2413	0.9993	0.008361	6.4688E-5
	55	α=392.0795, β=1.32937	0.9974	0.015445	2.5856E-4
	60	α=318.62, β=1.37483	0.9969	0.01748	3.36026E-4
	65	α=286.25739, β=1.31995	0.9986	0.01313	1.4881E-4
Two-term exponential	45	a=1.80906, k=0.00223	0.9981	0.01267	1.6803E-4
	50	a=1.78595, k=0.00287	0.9991	0.00935	8.0341E-5
	55	a=1.8590, k=0.00381	0.9961	0.01867	3.7746E-4
	60	a=1.89525, k=0.00479	0.9948	0.02247	5.5541E-4
	65	a=1.8585, k=0.00522	0.9977	0.01675	2.4722E-4
Wang and Singh	45	a=-0.00118, b=3.6108E-7	0.9996	0.00666	3.0989E-5
	50	a=-0.00157, b=6.48102E-7	0.9997	0.00518	2.26246E-5
	55	a=-0.00191, b=8.83899E-7	0.9996	0.005803	3.6373E-5
	60	a=-0.00233, b=1.29E-6	0.9994	0.007731	6.4252E-6
	65	a=-0.00267, b=1.8161E-6	0.9990	0.008896	1.16073E-4

Table 4. Fitting results of the combined drying experiment conditions Weibull model.

No.	Drying Methods	α	β	R^2	RMSE	χ^2
1	Microwave Vacuum	44.78224	1.37558	0.9967	0.07478	2.6689 E-4
	Hot air	10.21949	0.36361	0.9495	0.005565	5.16206E-5
2	Microwave Vacuum	15.69313	1.15368	0.9787	0.010596	0.00227
	Hot air	1.66766	0.2408	0.9418	0.013884	7.17954 E-5
3	Microwave Vacuum	27.61597	1.33834	0.9991	0.00637	8.60956 E-5
	Hot air	2.78942	0.23631	0.9528	0.005943	4.65088 E-5
4	Microwave Vacuum	27.96621	1.2897	0.9998	0.002696	1.53443 E-5
	Hot air	22.93173	0.33158	0.9209	0.017009	4.73052 E-4
5	Microwave Vacuum	27.18708	1.37423	0.9981	0.011923	1.77703 E-4
	Hot air	9.30512	0.49543	0.9771	0.014308	3.63677 E-5

Note: the test numbers (No.) corresponded to the experimental design in Table 1.

Linear regression analysis and variance analysis were performed by using Origin 8.0 software (OriginLab, Northampton, MA, USA). The experimental data obtained from microwave vacuum and hot air drying were used to fit the thin-layer drying models, resulting in coefficients, R^2, χ^2, and RMSE values for the three drying methods as illustrated in Tables 2, 3, and 4. The selection of the best model was based on a higher mean value of R^2 and a lower mean value of RMSE. The results showed that all four models were suitable for characterizing the drying process of star anise. During the process of microwave vacuum drying, the average R^2 values for the Lewis, Weibull distribution, two-term exponential, and Wang and Singh thin-layer drying models were 0.9703, 0.9968, 0.9939, and 0.9986, respectively, while the mean values of χ^2 were 0.00314, 0.0003375, 0.0005418, and 0.0001473, respectively. Both the Weibull distribution and Wang and Singh models exhibited a good fit. Considering model stability and the fact that the Weibull distribution function had fewer parameters and possesses explicit physical significance, it was selected to fit both the microwave vacuum and hot air stages of the combined drying phase. The average R^2 value for the microwave vacuum phase was 0.9945, while the hot air phase yielded an average R^2 value of 0.9484. The RMSE and χ^2 values were both close to zero, indicating that the Weibull distribution function provided an excellent fit for the segmented drying process involved in microwave vacuum combined with hot air drying.

Effective diffusion coefficient and activation energy

The drying process of star anise predominantly occurred in the falling rate drying stage. The complex internal moisture transport mechanism was described by using the moisture diffusion coefficient and calculated through Fick's diffusion equation (6). By substituting ln*MR*, star anise thickness *L*, and drying time *t* into the formula for fitting analysis, the slope of the equation led to the derivation of D_{eff}. With the rise of microwave intensity and temperature, D_{eff} showed an increasing trend. The range of D_{eff} in hot air drying was from 2.0386×10^{-8} to 4.8075×10^{-6} m^2/s, and in microwave vacuum drying, it ranged from 3.4423×10^{-7} to 8.8239×10^{-7} m^2/s. The D_{eff} value for microwave vacuum drying was significantly greater than that for hot air drying with a smaller D_{eff} value signifying a stronger binding force of star anise to its internal moisture. The increase in hot air temperature and microwave intensity caused the saturated vapor pressure on the surface of star anise to rise, enhancing the motion of water molecules per unit surface area, thereby promoting moisture migration and diffusion, and rendering the star anise more susceptible to drying. The rapid characteristic of microwave drying was evidently superior to hot air drying.

The Weibull distribution model could effectively simulate the combined microwave vacuum-hot air drying process. The β value during the microwave vacuum drying phase varied between 1.15368 and 1.37558, indicating a lag phase early in drying, with the drying process controlled by both internal and external moisture diffusion [16]. During the hot air drying stage, the β value ranged from 0.23631 to 0.49543, illustrating that drying was controlled by internal moisture diffusion. At a fixed temperature of 55℃ and a moisture content conversion of 30%, the D_{eff} value for both microwave vacuum and hot air phases was less than that at 3,000 W when the microwave power was 1,000 W. With a fixed microwave power of 2,000 W and a moisture content conversion of 30%, the D_{eff} value in the microwave vacuum phase was equivalent, whereas in the hot air drying stage at 65℃, the D_{eff} value was significantly lower than that at 45℃. Analysis suggested that as drying approached completion, the lower drying temperature reduced the ability for moisture diffusion within star anise, thus extending drying time. When the microwave power and drying temperature were fixed, the D_{eff} value at a 50% moisture content conversion was greater than 30%. Analysis indicated that, when dried to a 30% moisture content, the unobstructed internal pores of star anise under microwave exposure facilitated a rapid evaporation rate of water, promoting internal moisture diffusion in star anise, thereby increasing the effective diffusion coefficient value. Fitting Equations (7) and (8) provided the activation energies for microwave vacuum and hot air drying of star anise as 1.72435 kJ/mol·k and 42.19394 kJ/mol·k, respectively, which illustrated that microwave vacuum drying more readily removed internal moisture from star anise.

Analysis of trans-anethole and shikimic acid content

The primary component in star anise essential oil is trans-anethole, which is characterized by its volatile nature and thermal sensitivity. Exposure to high temperatures can exacerbate its volatilization, leading to a reduction in content. When the microwave power was at its minimum of 1,000 W, the contents of trans-anethole and shikimic acid were notably higher than that under other experimental conditions (Figure 3), which inferred that microwave heating could significantly shorten drying time, reducing the evaporation of trans-anethole. Simultaneously, drying at temperatures below 45℃ in a microwave vacuum environment ensured that the content of active ingredients was at its highest due to the rapid drying at low temperatures. In conditions where the converted moisture content was at 30%, and the hot air drying temperature was 55℃, the content of trans-anethole and shikimic acid at 1,000 W was increased by 15.6% and 40.77%, respectively, compared to that at 3,000 W. When the microwave power was fixed at 2,000 W and the hot air drying temperature was 45℃, the trans-anethole and shikimic acid content at a 30% converted moisture rate were increased by 14.7% and 9.3%, respectively, compared to 50%. It was evident that a lower converted moisture rate aided in the retention of active substances. A plausible explanation might be that the higher the drying degree in the microwave vacuum phase, the less time required for hot air drying, benefiting the preservation of active substances. When the microwave power was fixed at 2,000 W, and the converted moisture content was 30%, the trans-anethole and shikimic acid content at a hot air drying temperature of 45℃ were increased by 11.05% and 0.2%, respectively, compared to 65℃. While the temperature had a significant impact on the main content, the increase in shikimic acid was minimal. This observation could be attributed to the fact that at a wet base moisture content of 30%, drying was nearing completion, and the hot air's influence on star anise was limited. From the perspective of achieving the highest content of primary components, the optimal choice would be a microwave power of 1,000 W, a converted moisture rate of 30%, and a hot air drying temperature of 55℃. Combining these factors with the consideration of higher main component content and a shorter drying time, the best drying process was selected with a

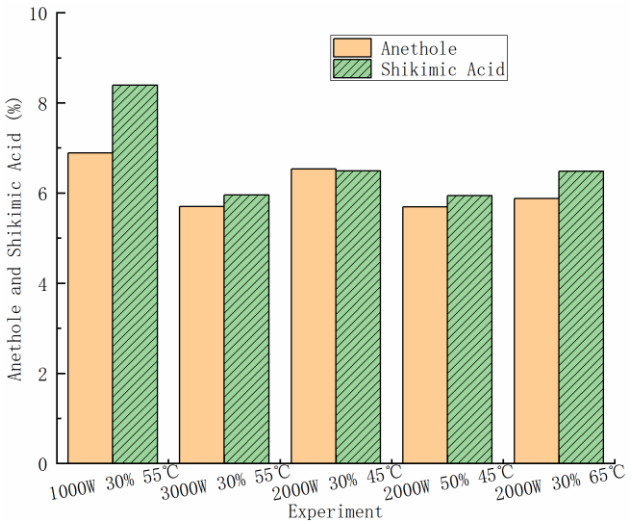

Figure 3. Impact of different experimental conditions on the content of trans-anethole and shikimic acid.

microwave power of 2,000 W, a converted moisture rate of 30%, and a hot air drying temperature of 45℃.

Conclusion

In this study, the star anise (*Illicium verum*) was taken as the subject, and various drying kinetic studies were performed by using microwave vacuum drying, hot air drying, and a combination of microwave vacuum and hot air drying methods. The findings revealed that both temperature and microwave power significantly impacted star anise drying kinetics. Specifically, the drying curve indicated that, at a microwave power of 1,000 W, the drying was controlled during the constant rate period, whereas, in the range of 1,500 to 3,000 W microwave power, the drying process was governed by the falling rate stage. Moreover, the drying rate increased with the increase in microwave intensity. The comparison of microwave drying with hot air drying showed that the drying time was reduced by over 93.6%, and the maximum drying rate was elevated by more than 22 times. Furthermore, four commonly used thin-layer drying models were employed to fit the drying process. Statistical results manifested that both the Weibull distribution and Wang and Singh models provided satisfactory fitting effects. Specifically, the Weibull distribution model exhibited an excellent fitting effect for the segmented drying process combining microwave vacuum and hot air. The contents of trans-anethole and shikimic acid were found to be significantly affected by hot air temperature and microwave power, presenting a declining trend with increasing temperature and microwave power. The lower moisture content in the conversion phase was favorable for retaining active ingredients. Balancing drying quality and efficiency, the optimal combined drying process parameters were determined as microwave power of 1,000 W, hot air temperature of 55℃, and conversion moisture content of 30%. For volatile oils which were thermosensitive and easily volatilized substances, the experiment had verified the feasibility of applying a segmented drying process that first used microwave vacuum followed by hot air for star anise drying. This research contributed a novel and reliable reference basis for the advancement of the star anise drying industry.

Acknowledgement

This study was supported by Research Starting Package for High-level Talents of Yulin Normal

University (Grant/Award Number: G2022ZK14), Yulin Scientific Research and Technology Development Program (Grant/Award Number: 202235127), and Guangxi Science and Technology Planning Project (Grant/Award Number: AD22080002).

References

1. Lv Q, Zhang YY, Ni H, Li HH. 2019. Extraction, separation and purification of anise oil and shikimic acid from star anise. J South China Norm Univ (Nat Sci Ed). 51(2):69-75.
2. Jin JL, Yuan Y, Dong J, Yang LW, Zhang XL, Wei J, *et al*. 2021. Moisture transformation and quality analysis of star anise during hot air drying. Sci Technol Food Ind. 42(14):79-85.
3. Monteiro RL, Link JV, Tribuzi G, Carciofi BAM, Laurindo JB. 2018. Microwave vacuum drying and multi-flash drying of pumpkin slices. J Food Eng. 232:1-10.
4. Zhao YT, Zhu HZ, Xu JX, Zhuang WJ, Zheng BD, Lo YM, *et al*. 2021. Microwave vacuum drying of lotus (*Nelumbo nucifera Gaertn*.) seeds: Effects of ultrasonic pretreatment on color, antioxidant activity, and rehydration capacity. Lwt-Food Sci Technol. 149:111603.
5. Ishibashi R, Numata T, Tanigawa H, Tsuruta T. 2022. *In-situ* measurements of drying and shrinkage characteristics during microwave vacuum drying of radish and potato. J Food Eng. 323:110988.
6. Ren YQ, Lei T , Sun DW. 2023. *In-situ* indirect measurements of real-time moisture contents during microwave vacuum drying of beef and carrot slices using terahertz time-domain spectroscopy. Food Chem. 418:135943.
7. Zhou Y, Liu YF, Li Q, Fan WY, Pan XL, Yu WX. 2023. Drying kinetics and heat mass transfer characteristics of thin layer pineapple during microwave vacuum drying. J Comput Methods Sci. 23(3):1165-1178.
8. Zang ZP, Huang XP, He CC, Zhang Q, Jiang CH, Wan FX. 2023. Improving drying characteristics and physicochemical quality of *Angelica sinensis* by novel tray rotation microwave vacuum drying. Foods. 12(6):1202.
9. Song CF, Wu T, Li ZF, Li J, Chen HY. 2018. Analysis of the heat transfer characteristics of blackberries during microwave vacuum heating. J Food Eng. 223:70-78.
10. Zhang ZY, Li YQ, Liu CH, Yan ZH, Zhu Y, Zhang YP, *et al*. 2020. Optimization of microwave drying of shiitake mushrooms considering thermal runaway. Food Sci. 41(10):230-237.
11. Gao MJ, Feng GQ, Zeng HC, Zeng J, Zhao A, Ma N. 2010. The impact of microwave drying on the effective components of *Panax notoginseng saponins*. J Chin Med Mater. 33(2):198-200.
12. Pu YY, Sun DW. 2017. Combined hot-air and microwave-vacuum drying for improving drying uniformity of mango slices based on hyperspectral imaging visualization of moisture content distribution. Biosyst Eng. 156:108-109.
13. Liu ZL, Staniszewska I, Zielinska D, Zhou YH, Nowak KW, Xiao HW, *et al*. 2020. Combined hot air and microwave-vacuum drying of cranberries: effects of pretreatments and pulsed vacuum osmotic dehydration on drying kinetics and physicochemical properties. Food Bioprocess Tech. 13(10):1848-1856.
14. Marzuki SU, Pranoto Y, Khumsap T, Nguyen LT. 2021. Effect of blanching pretreatment and microwave-vacuum drying on drying kinetics and physicochemical properties of purplefleshed sweet potato. J Food Sci Tech. 58(8):2884-2895.
15. Bozkir H. 2020. Effects of hot air, vacuum infrared, and vacuum microwave dryers on the drying kinetics and quality characteristics of orange slices. J Food Process Eng. 43(10):e13485.
16. Cheng XF, Pan L, Li N, Chen JQ. 2022. Moisture diffusivity characteristics and model fitting of jerusalem artichoke (*Helianthus tuberosus L*.) during microwave vacuum drying. Sci Technol Food Ind. 43(6):33-40.